# Is Additive Construction Ready for Seismic Regions? – A New Seismic Protective System Enabled by Additive Construction

Anthony Mackin, Jenna Migliorino, Hamdy Farhoud, and Islam M. Mantawy

Rowan University, Glassboro, NJ 08028, USA

mantawy@rowan.edu

**Abstract.** Conventional design for bridges in seismic-prone areas relies on ductility concept by concentrating the damage at columns' ends. This approach is adequate for life safety; however, bridge columns exhibit significant damage and residual deformations resulting in expensive repairs or the need for full replacement. Several seismic protective systems were developed over the last few decades to minimize the damage and enable repair after strong earthquakes like rocking systems, dampers, and seismic isolation systems. This paper proposes an innovative system that integrates several seismic protective concepts to achieve self-repair and deconstruction through additive construction. In this proposed system, protected elements such as bridge bent caps, columns, and footings are additively constructed. In addition, the columns are designed to rock at interfaces between the columns and bent cap/footing, and external elements are added to dissipate energy to promote resiliency.

**Keywords:** accelerated bridge construction, seismic, repair, deconstruction, additive construction

## 1 Introduction

Bridge design concepts in seismic-prone areas have been in place to ensure life safety by concentrating the damage at plastic hinges within the columns at beam/footing column connection to provide sufficient ductility. However, these design concepts do not account for functional recovery. Successful functional recovery boosts the economy, requires minimum to zero recovery time (rapidity), and achieves sustainability goals. This paper discusses how the functionality and rapidity benefits of several previously developed seismic protective systems can be integrated into a novel system that achieves zero functionality loss and zero downtime while accelerating construction. One of the methods of manufacturing that the authors explore further, for this integrated system, is the additive construction of all components of bridge bents. Zhang et al [1] developed a reinforced additively constructed wall specimen and tested the wall under quasi-static cyclic loading. Raza et al [2] also conducted experiments on prestressed segmental columns that used 3D-printed concrete as formwork for the column. Furthermore, other researchers have completed numerical simulations of 3D-printed concrete structures under seismic conditions. By additively constructing the new system, accelerated bridge construction can be further advanced. The system can be additively constructed in parts beforehand, then delivered to the site for assembly, and can be disassembled later, if needed. This paper integrated the benefits of the successful seismic protective system incorporating rocking systems, dampers, and seismic isolation systems.

## 2 Proposed Integral Seismic Protective System

The proposed integrated seismic protective system combines structural benefits from rocking columns, dampers, and seismic isolation, utilizing the best characteristics of each system. The integration of the benefits from each system presents a new solution for addressing earthquake protection. Additively constructed, post-tensioned rocking columns (1 in Figure 1) would allow the structure to rotate/rock freely during- and self-center after earthquakes. External energy dissipation devices (4 in Figure 1) would provide energy dissipation by rotational friction. Connection details (3 in Figure 1) inspired by seismic isolation's concave surface (2 in Figure 1) would help to reduce bearing stresses at the foundation and bent cap. Elastic or auxetic materials between column concave ends and foundation/bent cap would help absorb/dissipate more energy. Schematics of the new concept behind this novel system are shown in Figure 1. Figure 1b presents an alternate view of the system, showing the concave surface, the damping material, and the external energy dissipators reaching from the foundation to the additively constructed column. Figure 2 shows a schematic of the connection behaviour during seismic excitations.

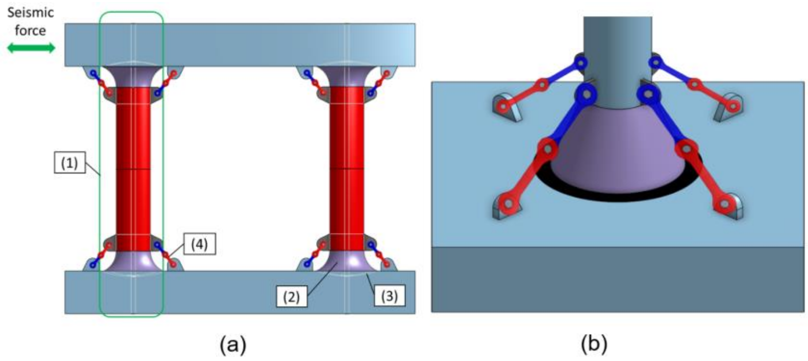


**Figure 1.** Preliminary Integrated Seismic Protect Systems (a) bent details, (b) connection details: (1) Additively Constructed Rocking Column, (2) Concave Surface Inspired by Seismic Isolation, (3) Damping/Auxetic Materials, (4) External Energy Dissipators

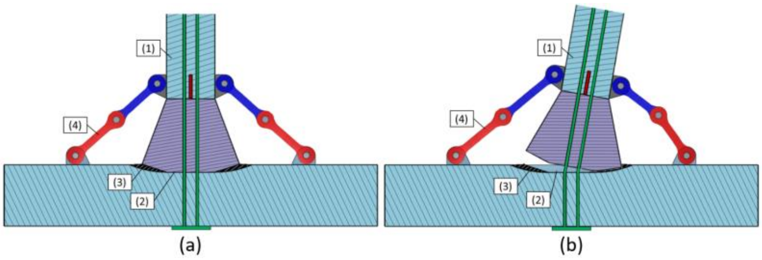


**Figure 2.** Rocking Column Top/Base Connection in the Combined System (a) Undeformed Configuration, (b) Deformed Configuration: (1) Additively Constructed Column, (2) Concave Surface Inspired by Seismic Isolation, (3) Damping/Auxetic Materials, (4) External Energy Dissipators

# 3 Materials

## 3.1 Concrete for Additive Construction

The developed concrete mixtures for additive construction consist of different binders including ordinary Portland cement (OPC-Type 1), Silica Fume (SF), and Fly Ash (FA), the latter two ingredients are supplementary cementitious (SCMs) as byproducts from other industries whereas the former is an emissive source responsible for 8% of global carbon emissions. Table 1 lists the different chemical compositions by chemical elements for all raw materials. Aggregate sizes for additive construction depend on the nozzle size to prevent clogging. Two different aggregate sizes were used: Type 1: fine grain sand and Type 2: medium grain to enable the mixture to conform to printability requirements (extrudability, buildability, and open time). Moreover, the presence of rheology-modifying admixtures in the mixture such as high-range water reducer (HRWR) and shrinkage-reducing admixture plays a crucial role in optimizing the properties of the mix in terms of strength, workability, durability, as well as extrudability.

**Table 1.** The chemical composition of used materials.

| Element | $SiO_2$ | $Fe_2O_3$ | $Al_2O_3$ | CaO | MgO | $SO_3$ | $K_2O$ | LOI |
|---|---|---|---|---|---|---|---|---|
| OPC (%) | 16.12 | 3.58 | 5.08 | 65.92 | 2.85 | 4.32 | 1.36 | 0.77 |
| Fly Ash (%) | 15.23 | 2.90 | 5.30 | 66.40 | 2.90 | 5.07 | 1.38 | 0.82 |
| Silica Fume (%) | 96.29 | 0.133 | 0.37 | 1.10 | 0.26 | 0.18 | 0.62 | 1.05 |
| Type 1 Sand (%) | 99.11 | -- | 0.714 | 0.047 | -- | 0.08 | 0.04 | 0.01 |
| Type 2 Sand (%) | 95.0 | 0.09 | 4.50 | 0.10 | -- | -- | 0.30 | 0.01 |

### 3.2 Mixing Procedure and Mixture Constituents

The mixture design matrix was prepared using a binder replacement ratio of 40 % of the OPC by weight with different percentages of SCMs (30% of OPC weight was replaced by FA and 10% of OPC weight was replaced by SF). The binder-to-aggregate ratio is 1:1 by weight and water-to-binder (W/B) ratio is 18% by weight, as shown in Table 2. The combined sand mixture consists of 50%Type 1: fine sand and 50% Type 2: medium sand. Additionally, HRWR and shrinkage-reducing admixture were added to the mixture with percentages ranging from 1.1% to 1.30%, and 1.4% of the total weight of the cementitious materials, respectively.

**Table 2.** Mixtures constituents' weights (kg/m3)

| ID | $H_2O$ | OPC | FA Type C | SF | Sand Type 1 | Sand Type 2 | HRWR | Shrinkage Reducing Admixture |
|---|---|---|---|---|---|---|---|---|
| M1 | 198 | 660.8 | 330.4 | 110.1 | 550.7 | 550.7 | 13 ± 1 | 15.4 |

The mixture was prepared by combining the dry constituents, namely binders, and sands, using a planetary mixer in dry conditions for 10 minutes. Subsequently, half of the high-range water-reducing (HRWR) admixture was added to the entire water quantity and manually stirred in a laboratory beaker. The resulting solution was then incorporated into the dry mixture and mixed for five minutes. Upon completing the initial five minutes of mixing, a shrinkage-reducing admixture was introduced to the mixture and mixed for three minutes. Finally, the remaining half of the HRWR was gradually added to the mixture for five minutes to ensure a uniformly printable consistency.

For the optimal formulation suitable for printing, it was crucial to maintain a flow table diameter within the range of 100 to 150 millimeters to ensure adequate flowability and extrusion. The consistency of layer extrusion during printing, ensuring uniform layer thickness and width, was achieved by controlling the extrusion rate. The printer tube (Section 4) was loaded with developed and manually compressed using a steel rod to eliminate any potential presence of air bubbles. Simultaneously, cubes with dimensions of 50*50*50 cubic millimeters were prepared both before and after the printing process using printable concrete. These cubes were compacted in two layers on a vibrating table, with each layer subjected to 10 seconds of vibration. The demolding of all cast cubes took place after a one-day curing period.

### 3.3 Testing Methods and Results for Fresh and Hardened Properties

The mechanical properties were evaluated solely for compressive strength in the printable material, utilizing cube specimens measuring 50 x 50 x 50 cubic millimeters. Two distinct scenarios were considered: the first before loading the printing tube and initiating the printing process, and the second after extracting the material from the tube and completing the printing process. Compressive strength tests for the printable high-strength mortar cubes were conducted at three, seven, and 28 days. The testing outcomes, encompassing compressive strength in accordance with ASTM C109-20 [3], flow table performance in accordance with ASTM C 1437-07 [4], and Vicat test results in accordance with ASTM C191-21 [5] for the developed high-strength concrete mix, are presented in Table 3. These tests were carried out at the Additive and Robotic (ARC) laboratory at Rowan University. Notably, the printing mix exhibits an open time exceeding 60 minutes when confined within the printing tubes, a flow of 114 mm, and a compressive strength of at least 47 MPa in just three days.

**Table 3.** Testing results of fresh and hardened properties.

| Printing Process | Compressive Strength (MPa) | | | Flow table (mm) | Vicat (min) | |
|---|---|---|---|---|---|---|
| | 3 days | 7 days | 28 days | | Initial setting time | Final Setting time |
| Before | 48.4 | 52.9 | 68.9 | 114 | 61 | 180 |
| After | 47.5 | 53.7 | 64.1 | Not Measured | | |

## 4 Printability of the 3D-Printed Mixes

ARC Lab hosts additive construction systems. The 3D printer is a combined system "Scara Elite Roadrunner", Figure 3. The combined system includes (1) a Scara Elite printer, 2) a rail track, and 3) a concrete pump. The maximum operational space of the combined system at one set-up is W=2.95 meters. L=7.06 meters. H=2.54 meters. The printer is capable of printing at an average speed of 30 to 100 mm per second. The 3D-printing system is equipped with different nozzle sizes ranging from 6 mm to 50 mm. The concrete pump operates continuously on 220V service.

In additive construction, both the construction material (mainly concrete) and equipment differ from those in conventional construction. Materials for conventional construction provide specific flowability (slump) to fill up the formwork and encapsulate the reinforcement. In contrast, materials for additive construction conform to printability requirements [6]. Figure 4 presents the printability requirements for concrete additive construction including extrudability, open time, buildability, and pumpability. Extrudability: the "*ability of the material to be smoothly ejected through the printing nozzle without inducing blockage of the conduits or significant damage to the material quality*" [6]. Figure 4-a shows the continuous printing of concrete for castle-like structures with complex printing paths including straight lines, curved lines, chamfer, and sharp turns. Open Time: "*time in minutes needed for the mixture to maintain good extrudability without disruption and loss of extrudability and buildability*" [6]. Figure 4-b shows flow table testing to measure open time over time intervals. Buildability or Shape Stability: the “*ability of a print to preserve vertical and lateral stability under increasing loads due to superimposed/subsequent layers with controlled deformation*” [6]. Figure 4-c shows successful extrusion but significant interlayer buildability failure, whereas Figure 4-d shows successful printing of a concave structure with a slope of around 30 degrees. Pumpability: the ability to continuously pump fresh concrete mixtures delivered through a closed hose system under pressure.

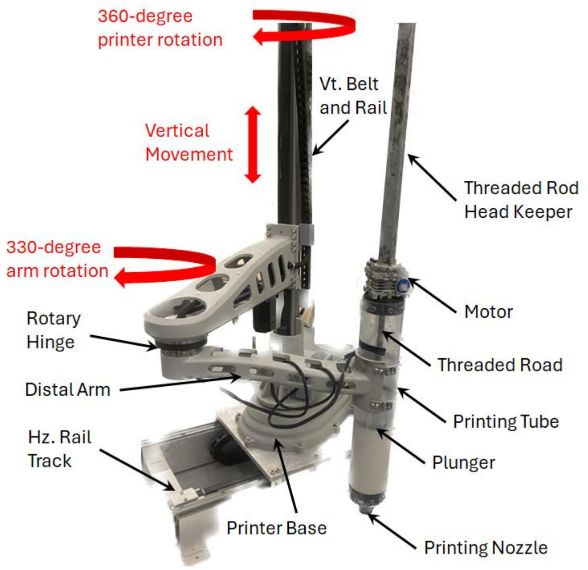


**Figure 3.** 3D-printing equipment at ARC-Lab at Rowan University.

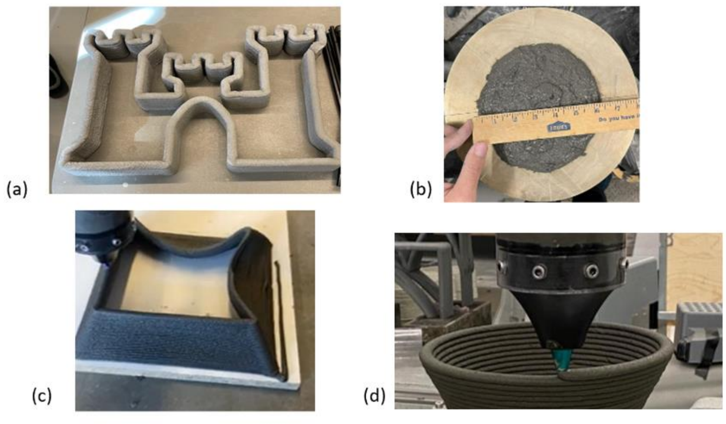


**Figure 4.** Additive Construction Printability Requirements (a) Extrudability; (b) Open Time; (c) Buildability Failure; and (d) Buildability Success

## 5 Additive Construction of Column Shell

A component design is currently being developed based on several previous designs, such as the integrated seismic protective system, as well as from a previous study [7]. In addition to developing an entire bent with two columns, the model for component testing consists of one foundation and one column end, as depicted earlier in Figure 2. The seismic forces will be simulated using an actuator attached to the top of the column or a shake table to which the foundation is attached. Additionally, this design is scaled down from a previous model from Mantawy and Thonstad [7-8]. While the goal is to develop a system like this model in the future (Figure 1-a), a smaller model is required to verify the concept in component testing. Figure 2 shows a cross-section of the combined system component in both an undeformed and deformed configuration. Developing a smaller, component model instead of a full-scale model allows for the simulation of the seismic forces without the need for larger testing equipment. In the future, larger equipment will be required to simulate the full effect of seismic forces, but at the moment, utilizing component testing confirms the intended performance and response before full-scale testing.

Another unique design for the connection testing is the utilization of 3D-printed concrete for the foundation and column with Ultra-High-Performance Concrete (UHPC) using Additive Construction. Additive Construction is a cost- and material-efficient process that can be implemented into the design of the integrated system. The flared column/column end was successfully printed using the developed 3D-printed materials in this paper, as shown in Figure 5. The column diameter is 150 millimeters with an overall height of 610 millimeters. The flared end diameters range from 150 millimeters to 200 millimeters. The 3D-printing of this column shape poses challenges due to the steep slopes; however, the 3D-printed material was capable of holding the slopes without any interlayer failures.

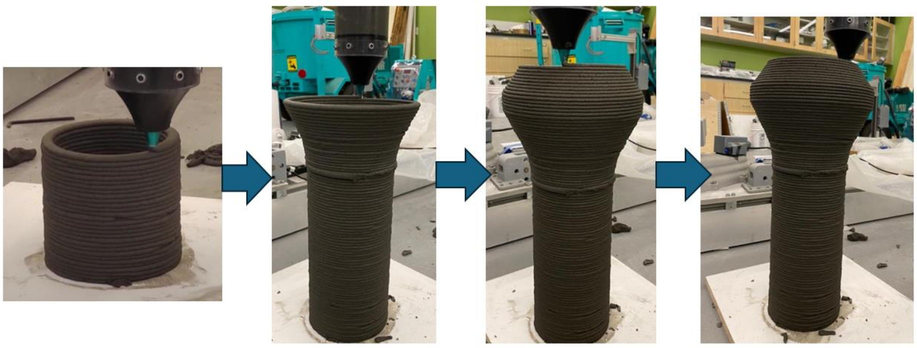

**Figure 5.** Additive Construction of 3D-Printed Concrete Shell.

## 6 Summary

The integration of benefits of current seismic protection systems can result in superior systems that enable damage-free, full functional recovery, and zero downtime and change the definition of resilience to beyond resilience. The system also enables the use of damage-free elements without hindering energy dissipation. In case of major earthquakes, the system offers replacement of each component. A smaller, component design of the system has been developed at Rowan University. Preliminary results showed the feasibility of the system to be constructed even with steep slopes. In the future, the system will need to be scaled up to a previous model from Mantawy, Thonstad [7], which will present unique challenges with additive construction and assembly of the system.

## 7 Acknowledgement

This work was made possible by a U.S. Department of Education Graduate Assistance in Areas of National Need (GAANN) Grant Number P200A210109.

## References

1. Zhang, D., Feng, P., Zhou, P., Xu, W., & Ma, G. (2023). 3D printed concrete walls reinforced with flexible FRP textile: Automatic construction, digital rebuilding, and seismic performance. Engineering Structures, 291, 116488.
2. Raza, S., Triantafyllidis, Z., Anton, A., Dillenburger, B., & Shahverdi, M. (2024). Seismic performance of Fe-SMA prestressed segmental bridge columns with 3D printed permanent concrete formwork. Engineering Structures, 302, 117423.
3. ASTM, C. (2020) Standard Test Method for Compressive Strength of Hydraulic Cement Mortars (Using 2-in. or [50-mm] Cube Specimens). C109.
4. ASTM, C. (2007). Standard test method for flow of hydraulic cement mortar. C1437.
5. ASTM, C. (2021) Standard Test Methods for Time of Setting of Hydraulic Cement by Vicat Needle. C191.
6. ISO/ASTM 52939; Additive Manufacturing for construction — Qualification principles — Structural and infrastructure elements. ISO/ASTM: Geneva, Switzerland, 2022.
7. Thonstad, T., Mantawy, I. M., Stanton, J. F., Eberhard, M. O., and Sanders, D. H., Shaking Table Performance of a New Bridge System with Pretensioned Rocking Columns. Journal of Bridge Engineering, 2016. 21(4): p. 04015079.
8. Mantawy, I. M., Thonstad, T., Sanders, D. H., Stanton, J. F., and Eberhard, M. O., Seismic Performance of Precast, Pretensioned, and Cast-in-Place Bridges: Shake Table Test Comparison. Journal of Bridge Engineering, 2016. 21(10): p. 04016071.